Steering Law Design for Redundant Single-Gimbal Control Moment Gyroscopes

Nazareth S. Bedrossian,* Joseph Paradiso,† and Edward V. Bergmann‡
Charles Stark Draper Laboratory, Inc., Cambridge, Massachusetts 02139
and
Derek Rowell§
Massachusetts Institute of Technology, Cambridge, Massachusetts 02139

Two steering laws are presented for single-gimbal control moment gyroscopes. An approach using the Moore-Penrose pseudoinverse with a nondirectional null-motion algorithm is shown by example to avoid internal singularities for unidirectional torque commands, for which existing algorithms fail. Because this is still a tangent-based approach, however, singularity avoidance cannot be guaranteed. The singularity robust inverse is introduced as an alternative to the pseudoinverse for computing torque-producing gimbal rates near singular states. This approach, coupled with the nondirectional null algorithm, is shown by example to provide better steering law performance by allowing torque errors to be produced in the vicinity of singular states.

I. Introduction

A MOST difficult problem for spacecraft attitude control using single-gimbal control moment gyroscopes (SGCMG) to provide control torques is the design of an effective steering algorithm. The major objective for any successful approach has been the avoidance of singular states that preclude torque generation in a certain direction, the singular direction. This situation occurs when all individual CMG torque outputs are perpendicular to this direction, or equivalently, the individual momenta have extremal projections onto this direction. These conditions, if not properly addressed, severely limit the usable momentum capability of the CMG system. Although the extra degrees of freedom provided by adopting redundant CMG systems may reduce the possibility of encountering singular states, singular configurations cannot be eliminated. These systems, however, usually possess alternative nonsingular configurations for any given total momentum state. More important, hardware-imposed limits on gimbal rates require that neighborhoods of singular states also must be considered in the steering law design. Ultimately, a candidate algorithm must be both real-time and hardware realizable.

In general, there are many ways to structure kinematic redundancy resolution methods. In reviewing various steering algorithms, the correspondence between SGCMGs and robotic manipulators[1] will be exploited to also include methods presented in the robotics literature. In this paper, these will be divided into two categories depending on the differential level where the inversion is accomplished. Recall that the forward kinematics for the CMG system is represented by a continuous, nonlinear, differentiable, vector-valued mapping, $f\colon T^n \to H \subset \mathbb{R}^3$, which can be written as

$$\boldsymbol{h}(t) = \boldsymbol{f}[\boldsymbol{\theta}(t)] \tag{1}$$

where $\boldsymbol{h}(t)$ denotes the total CMG momentum in spacecraft frame of reference, and $\boldsymbol{\theta}(t)$ are the gimbal angles. The first category is the inverse kinematic problem (IKP), which solves Eq. (1). One way of resolving the redundancy is to transform the IKP to a constraint optimization problem by suitable choice of performance index $p(\boldsymbol{\theta})$. This problem may be solved by the method of Lagrange multipliers. From the necessary conditions for a stationary point, $n+3$ independent nonlinear equations in the $n+3$ unknown gimbal angles and Lagrange multipliers are obtained, which can be solved by numerical methods. In this way, the singularity problem is handled directly since nonsingular gimbal angle configurations are generated for each momentum state. The IKP problem can be also cast as a trajectory tracking problem in control theory using Lyapunov techniques. This approach has been used for redundant manipulators in Refs. 2–4.

The second category of redundancy resolution methods involves the differential relationship between gimbal angle and momentum space coordinates:

$$\dot{\boldsymbol{h}} = \boldsymbol{J}[\boldsymbol{\theta}(t)]\dot{\boldsymbol{\theta}}(t) \tag{2}$$

These are called local inversion or tangent methods, and they require the solution of the under-determined system of linear equations (2). In this case redundancy is resolved by proper choice of the homogeneous solution, since all solutions to Eq. (2) can be expressed as[5]

$$\dot{\boldsymbol{\theta}} = \dot{\boldsymbol{\theta}}_P \oplus \dot{\boldsymbol{\theta}}_H$$

where $\dot{\boldsymbol{\theta}}_P$ is the particular solution ($\boldsymbol{J}\dot{\boldsymbol{\theta}}_P = \dot{\boldsymbol{h}}$), and $\dot{\boldsymbol{\theta}}_H$ is the homogeneous solution ($\boldsymbol{J}\dot{\boldsymbol{\theta}}_H = 0$) that represents nontorque-producing displacements usually referred to as null motion, and $\oplus$ is the direct sum. Of course, higher derivatives can also be used to resolve redundancy. The main operational difference between the two methods is that for a given momentum trajectory, the first method solves the optimization problem at momentum intervals, generating gimbal angle solutions that can be "differentiated" to produce gimbal rate commands, whereas the local method solves the differential relationship at time intervals, generating gimbal rate solutions that can be integrated to generate the momentum trajectory. For an excellent general discussion of these two approaches see Ref. 6. In this paper only local methods will be considered.

Received March 10, 1989; revision received Aug. 18, 1989.

*Graduate Student, Department of Mechanical Engineering, Massachusetts Institute of Technology.

†Member of Technical Staff.

‡Section Chief, Flight Systems.

§Associate Professor, Department of Mechanical Engineering.

In reviewing local methods, we will only be concerned with single degree of redundancy systems, i.e., where the dimension of the nonsingular Jacobian nullspace is one. For these systems, local methods involve choosing only two quantities: the magnitude and sign of the null vector (i.e., the homogeneous solution). Most local methods solve Eq. (2) exactly, where the particular solution $\dot{\theta}_P$ is formed from the Moore-Penrose pseudoinverse. The simplest method is to just use the pseudoinverse, which generates gimbal rates that minimize their quadratic cost, i.e., $(\|\dot{\theta}\|_2)^2$. This method, however, does not generate gimbal angle trajectories that avoid singular configurations. A proof of this fact, in the context of robotic manipulators, can be found in Ref. 7. A most common remedy is to choose the homogeneous solution to instantaneously maximize a scalar performance criterion $p(\theta)$. These are called gradient methods, an example of which is the inverse determinant avoidance law.[8] These methods also cannot guarantee singularity avoidance, since the performance index is not usually a monotonic function of the gimbal angles, thus instantaneously maximizing this function leads to local extrema that can be singular configurations. Equivalently, the projection of the particular solution onto the gradient of $p(\theta)$ can be negative and may dominate $\dot{p}(\theta)$ (i.e., $\dot{p} = \nabla p \cdot \dot{\theta}_P + \nabla p \cdot \dot{\theta}_H$), resulting in a net decrease in the value of $p(\theta)$. A different approach applied to a four-pyramid CMG system is the maximum gain method.[9] Null motion is added in the direction of maximum global gain, and singular states are avoided by using a lookup table of parameters that is generated by off-line calculation and reduced somewhat by taking advantage of system symmetry.

Two singularity avoidance steering laws, the "direct" method, which introduces null motion to steer away from the most rapidly approaching singularity, and the "indirect" method, which adds null motion to steer toward the saturation singularity, are presented in Ref. 8 for a six-pyramid CMG system. This paper is noteworthy for the fact that gimbal rate limits were also considered in evaluating the performance of the proposed methods, which were successful in avoiding internal singularities. For the four-pyramid system shown in Fig. 1, however, the indirect method was unable to avoid[13] the elliptic (singular configuration where null motion is impossible[1]) internal singularity discussed in Sec. III. One other approach that is based on instantaneously optimizing an objective function is to assign gimbal rates via linear programming.[10] The advantages of this approach are that performance criteria such as rate limits, hardware failures, and variations in CMG system definition can be explicitly taken into account. Due to the use of a gradient-based objective, however, singularity avoidance is not guaranteed for SGCMG systems.

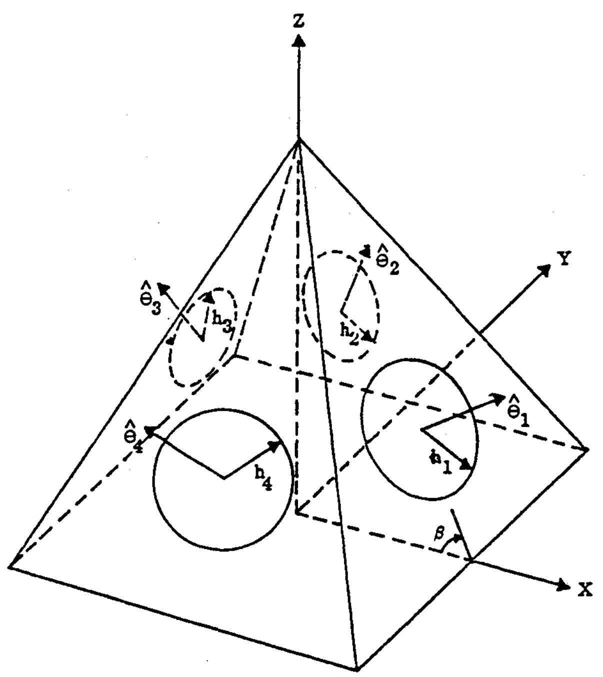

Fig. 1 Four-pyramid-mounted SGCMG system.

Another approach is to resolve redundancy by introducing additional constraint functions of the form $c(\theta) = 0$. In general, as many constraints as degrees of redundancy would be necessary. In the case of four SGCMGs, only one constraint would be required. Optimization of objective functions can also be posed in this form. Augmenting these constraints with Eq. (1), the problem reduces to the solution of

$$f[\theta(t)] = h(t) \tag{3a}$$

$$c[\theta(t)] = 0 \tag{3b}$$

To solve Eq. (3) by local methods requires solving the differential relationship:

$$\begin{bmatrix} D[f[\theta(t)]] \\ D[c[\theta(t)]] \end{bmatrix} \dot{\theta}(t) = \begin{bmatrix} \dot{h}(t) \\ 0 \end{bmatrix} \tag{4}$$

where $D[\cdot]$ denotes the differential operator. This approach is referred to as the extended Jacobian method after Ref. 11, where the choice of constraint function is Eq. (7). For a unique solution to Eq. (4), the extended Jacobian must be nonsingular along the entire path. In general, this condition may not be satisfied.

Two different local redundancy resolution methods are presented in the following sections. The first method solves Eq. (2) exactly, using a unidirectional homogeneous solution, whereas the second approach solves Eq. (2) approximately in the vicinity of singular configurations.

II. Null-Motion Algorithm

From various simulations using gradient-type methods, dynamically manipulating the direction of null motion to instantaneously maximize some performance criteria was found to be ineffective in avoiding internal singularities. This is due to the tendency of tangent-based methods to lock into gimbal angle trajectories of locally optimal performance criteria that can actually lead to singular configurations. Based on this observation, a new nondirectional null-motion algorithm using the Moore-Penrose pseudoinverse $J^+ = J^T[JJ^T]^{-1}$ was found to be more successful in avoiding certain elliptic-type internal singularities. The principal features of this approach are the nondirectional nature of the homogeneous solution and the fact that, unlike other methods, substantial null motion is introduced even when the system is far from being singular. In effect, null motion of varying degrees is always applied. The aim of this strategy is to prevent the gimbal angle trajectory from settling into locally optimal configurations, which may eventually result in a singularity. With this approach the solution to Eq. (2), assuming unit momentum magnitudes, is given by

$$\dot{\theta} = J^+\dot{h}(t) + \lambda(\theta)n \tag{5}$$

where

$$\lambda(\theta) = \begin{cases} m^6 & \text{if } m \geq 1 \\ m^{-6} & \text{if } m < 1 \end{cases}$$

$m = \sqrt{\det(JJ^T)}$, singularity measure

$n = \dfrac{\partial h_1}{\partial \theta} \wedge \dfrac{\partial h_2}{\partial \theta} \wedge \dfrac{\partial h_3}{\partial \theta} = [C_1, C_2, C_3, C_4]$, Jacobian null vector

$C_i = (-1)^{i+1}M_i$, order 3 Jacobian cofactor

$M_i = \det(J_i)$, order 3 Jacobian minor

J_i = J with ith column removed
$\dot{h}(t)$ = torque request

Here, n represents the one-dimensional Jacobian null-space-basis vector. This vector is generated using the generalized cross or wedge product[12] $\wedge$ to form the vector orthogonal to the three Jacobian row vectors.[13] This choice of scaling factor λ arises from the representation of m as a measure of distance from singularity, as well as the fact that the magnitude of the nonsingular Jacobian null vector n is identical to m, i.e.,

$$\det(JJ^T) = \langle n, n \rangle \tag{6}$$

The null vector must thus be normalized before it is used in the steering algorithm, so as not to degrade the effectiveness of null motion as the system approaches a singularity and m decreases. This fact follows directly from the following proposition.

Proposition: Given the linearly independent vectors $v_1, \ldots, v_{n-1} \in \mathbb{R}^n$, let $w = v_1 \wedge \cdots \wedge v_{n-1}$. Then

$$\langle w, w \rangle = \det(G)$$

where

$$G = \text{gram matrix}$$
$$G_{i,j} = \langle v_i, v_j \rangle$$

The validity of Eq. (6) is easily deduced by applying the Binet-Cauchy formula[14] to Eq. (6), i.e.,

$$\det(JJ^T) = \sum_{i=1}^{4} M_i^2$$

and performing the indicated inner product of the null vector as defined in Eq. (5).

Although this approach has the advantage that it does not constrain null motion to instantaneously maximize a performance criterion, such as m, it has two potential shortcomings.

1) Null motion is added to the solution without regard to whether it can instantaneously affect the value of m (i.e., gimbals are locally redistributable). The gimbals are not locally redistributable when

$$\frac{\partial m}{\partial \theta} \cdot n = 0 \tag{7}$$

This is also the necessary condition for a stationary point of $m(\theta)$ subject to the constraint $h = f(\theta)$.

2) Since the direction of null motion is not prescribed, it may actually decrease m, thus inadvertently steering toward a singularity.

This latter adverse property, however, must be evaluated in the proper perspective. The pseudoinverse itself is actually the mechanism that drives the system to a singular configuration. The reason for this can be attributed to the two-norm minimization nature of the pseudoinverse solution, which tends not to move inefficiently oriented gimbals since that would increase the two norm of the gimbal rates. This fact is easily seen from the negative projection of the particular solution on the gradient of m,

$$\frac{\partial m}{\partial \theta} \cdot \dot{\theta}^{+} < 0 \tag{8}$$

where $\dot{\theta}^{+} = J^{+}\dot{h}(t)$. If Eq. (8) remains zero during a time when the null projection is negative, any singularity that is reached by null motion is escapable by definition. This condition, however, is not usually satisfied, and consequently this approach also does not guarantee singularity avoidance.

III. Singularity Robust Inverse

It has been seen that the particular solution produced by the pseudoinverse eventually drives or restricts the system to singular configurations. Since solving Eq. (2) exactly can drive the system to a singularity, one might surmise that it may be possible to avoid singularities if small torque errors are allowed. One method of accomplishing this is provided by the singularity robust inverse (SR inverse) proposed for robotic manipulators in Refs. 15 and 16 as an alternative to the pseudoinverse. A similar method, the "transpose steering law," had been proposed in Ref. 17 for double-gimbal CMGs. Using the SR-inverse method, an approximate output torque close to the desired torque can be generated, even when the Jacobian is singular. A tradeoff is accomplished between solving the torque equation exactly (accuracy of solution) and minimizing the gimbal rates (feasibility of solution). Near a singular configuration, gimbal rates remain finite and bounded in exchange for a buildup of torque error. The SR inverse is obtained by solving the combined minimization problem:

$$\min_{\dot{\theta}} P = 0.5 e^T K e$$

where

$$e = \begin{bmatrix} \dot{h} - J\dot{\theta} \\ \dot{\theta} \end{bmatrix}$$

$$K = \begin{bmatrix} K_1 & 0 \\ 0 & K_2 \end{bmatrix}$$

Here $K_1 > 0$ and $K_2 > 0$ are weighting matrices. The unique minimizing solution is obtained from

$$\frac{\partial P}{\partial \dot{\theta}^T} = K_2\dot{\theta} - J^T K_1 \dot{h} + J^T K_1 J \dot{\theta} = 0 \tag{9}$$

and is given by

$$\dot{\theta}^{*} = [J^T K_1 J + K_2]^{-1} J^T K_1 \dot{h} = J^{*}\dot{h}$$

where J^{*} is the SR inverse. Setting $K_1 = I$, $K_2 = kI$, it can be shown that

$$\dot{\theta}^{*} = J^T[JJ^T + kI]^{-1}\dot{h}$$

also satisfies Eq. (9), and the SR inverse can be expressed as

$$J^{*} = J^T[JJ^T + kI]^{-1} = [J^T J + kI]^{-1} J^T$$

It can be easily shown that the particular solution obtained from this method is still orthogonal to the homogeneous solution. Since the SR solution lies in the row space of the Jacobian, as does the pseudoinverse, it is expected that the SR-inverse approach will have similar singularity avoidance properties as far as elliptic-type internal singularities are concerned. The robustness properties are determined by the scaling factor k, which expresses the tradeoff between exactness and feasibility of solution. It is seen that the pseudoinverse is identical to the SR inverse when $k = 0$. For small values of k, small error is introduced in the torque solution, and large rate magnitudes are still produced in the neighborhood of singular states. For larger k values, torque error increases and the magnitude of calculated gimbal rates decline.

The SR-inverse approach, however, is not without shortcomings. The most crucial problem is that if the system does become singular, and a torque is requested along the singular direction, the SR inverse is unable to generate nonzero gimbal rates. The system could then be trapped in the singular state. This property is evident from the expression of J^{*} in terms of the singular value decomposition (SVD) of the Jacobian matrix

$$J = U\Sigma V^T \tag{10}$$

where

$$\Sigma = [\Sigma_{MP} 0]$$

$$\Sigma_{MP} = \text{diag}(\sigma_i), \qquad i = 1, \ldots, 3$$

where σ_i, are the non-negative Jacobian singular values. Using Eq. (10), it can be shown that

$$J^* = V\Sigma^* U^T$$

where

$$\Sigma^* = \begin{bmatrix} \Sigma_{SR} \\ 0^T \end{bmatrix}$$

$$\Sigma_{SR} = \text{diag}\left(\frac{\sigma_i}{\sigma_i^2 + k}\right) \qquad i = 1, \ldots, 3$$

If $\dot{h}$ lies along one of the column vectors of U, say u_i, the gimbal rates computed by the SR inverse are given by

$$\dot{\theta}^* = \frac{\sigma_i}{\sigma_i^2 + k} v_i \tag{11}$$

where v_i is the ith column of V. From Eq. (11), it is seen that if one of the singular values, σ_i, is zero and the torque request is along the corresponding singular vector u_i, the computed gimbal rates are zero. Unless this singularity allows for escape by null motion, there is no possibility of removing the system from the singular configuration. This serves to illustrate that the singular direction categorizes singular states beyond the mere fact of their existence and should be considered in robust CMG steering laws. The reason for this is that solution gimbal rates can always be calculated for torque requests that lie in the range of the transformations J^+ or J^*. In the SR-inverse case, as long as the desired torque is not exactly aligned with the singular direction, finite torque-producing gimbal rates can be calculated; whereas for the pseudoinverse, the desired torque must be orthogonal to the singular direction (i.e., must lie in the plane spanned by the nonsingular columns of J) in order to compute finite torque-producing rates.

To overcome the problems of conflicting requirements on the value of the weighting factor, it was made a function of the singularity measure. In this way, k will have a large value near singularities, and a small or zero value away from singularities. The weighting factor was chosen in the following manner:

IF $m > m_{CR}$ THEN

$k = 0$

ELSE

IF $\dfrac{k_0}{m} < k_{max}$ THEN

$k = \dfrac{k_0}{m}$

ELSE

$k = k_{max}$

where

m_{CR} = critical value of m
k_0 = constant
k_{max} = maximum value of weighting factor

In this fashion, the weighting factor is adjusted according to distance from singularity by inversely scaling it with the singularity measure. No error is introduced far from singularities, and the maximum error is limited by k_{max}.

IV. Simulation Results

In this section, simulation results are presented for the two candidate steering algorithms. For simulation purposes, a standard pyramid mounting arrangement of four single gimbal CMGs was chosen as shown in Fig. 1. The pyramid skew angle β was set at 54.73 deg to yield a symmetric three-axis momentum envelope. Software was written in double precision Fortran 77, and the CMG kinematics were integrated at a simulation interval of 0.01 s, using the routine DIVPRK, a Runge-Kutta-Verner fifth- and sixth-order method, from the International Mathematical and Statistical Library. The momentum magnitudes were set equal to unity, and the initial gimbal angles for all simulations were 0 deg. No direct rate limits were imposed, but the magnitude of the null constant λ was limited to $\lambda \le 3$ to prohibit excessive null motion. The torque-producing gimbal rates were computed using the dyadic approach.[18] To evaluate the performance of the various algorithms, we will adopt a gimbal rate limit of 2 rad/s as in Ref. 8. For tests using the SR inverse, the critical value was $m_{CR} = 1.0$, with constant $k_0 = 0.1$. The scaling factor was limited to $k_{max} = 0.2$.

To illustrate the singularity avoidance properties of the two algorithms, a constant torque request along the X axis is requested, i.e., $\dot{h} = [1, 0, 0]^T$. This direction is chosen because it will force the CMG system through the elliptic internal singularity at $h = [1.15, 0, 0]^T$ described in Ref. 1. Note that this singularity represents a worst case since it is an unescapable singularity, and the torque request is aligned with the singular direction. This singularity is not avoided using readily implementable existing algorithms.[13]

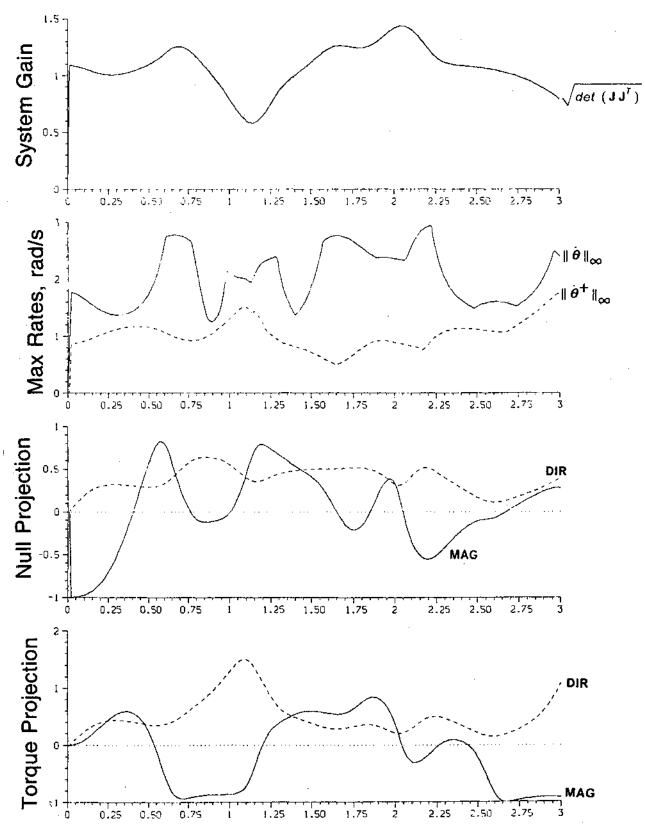

Fig. 2 Simulation results for null algorithm (X direction).

Simulation results for the nondirectional null algorithm [i.e., Eq. (5)] are shown in Fig. 2, where it is seen that the singularity is avoided since the singularity measure $m = \sqrt{\det(JJ^T)}$ remains nonzero for the entire simulation. From the maximum absolute gimbal rate plot (where the dotted curve represents the maximum gimbal rate from the pseudoinverse solution $\|\dot{\theta}^+\|_\infty$, and the solid curve represents the maximum total gimbal rate including the contribution of the homogeneous solution $\|\dot{\theta}^+ + \lambda n\|_\infty$), however, it can be seen that substantially high rates that violate the rate limit were generated. It is noticed that a large fraction of the rates are due to null motion introduced via the homogeneous solution. The nonzero null projection onto the singularity measure m [i.e., $\nabla m \cdot n$, with MAG $= |\nabla m \cdot n|$, and DIR $=$ sign$(\nabla m \cdot n)$] indicates that the gimbal angle trajectory generated by this method is not locally optimal. In addition, for $t < 0.5$ s, the singularity measure is decreasing due to the negative null projection while the torque projection [i.e., $\nabla m \cdot \dot{\theta}^\#$, with MAG $= |\nabla m \cdot \dot{\theta}^\#|$, and DIR $=$ sign$(\nabla m \cdot \dot{\theta}^\#)$] was positive, which would tend to increase m. Similarly, for $0.75 < t < 1.25$ s, the negative torque projection results in decreasing the singularity measure.

This same torque profile was used for the SR inverse only (no null motion), with results shown in Fig. 3. The plots clearly show that the elliptic singularity is not avoided, as was expected. Even though the system becomes singular, the SR matrix $[JJ^T + kI]$ remains nonsingular. This illustrates the fundamental property of the SR inverse; gimbal rates can still be computed even when the Jacobian is singular. This example also illustrates the fundamental shortcoming of this method discussed previously; calculated gimbal rates can decrease near singular states when the commanded request is aligned with the corresponding singular direction, as can be seen from the decreasing magnitude of the plotted maximum gimbal rate. All SR-resultant torque error (i.e., $\Delta T = T_{des} - T$) was in the commanded direction, thus off-axis torque errors did not perturb the momentum trajectory. When coupled with a gradient null motion algorithm, however, the SR inverse was able to avoid this singularity.[13] This was due to the fact that the SR inverse reduced the system response in the commanded direction, which thus allowed more time for null motion to be effective. Better performance, in terms of reduced torque errors, was obtained for the SR inverse with the nondirectional null algorithm shown in Fig. 4.

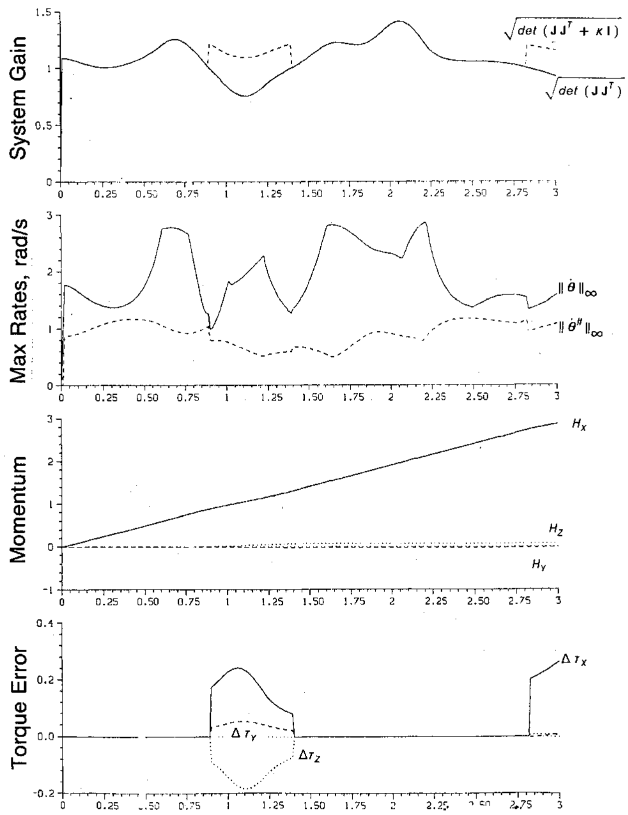

Fig. 4 Simulation results for SR with null algorithm (*X* direction).

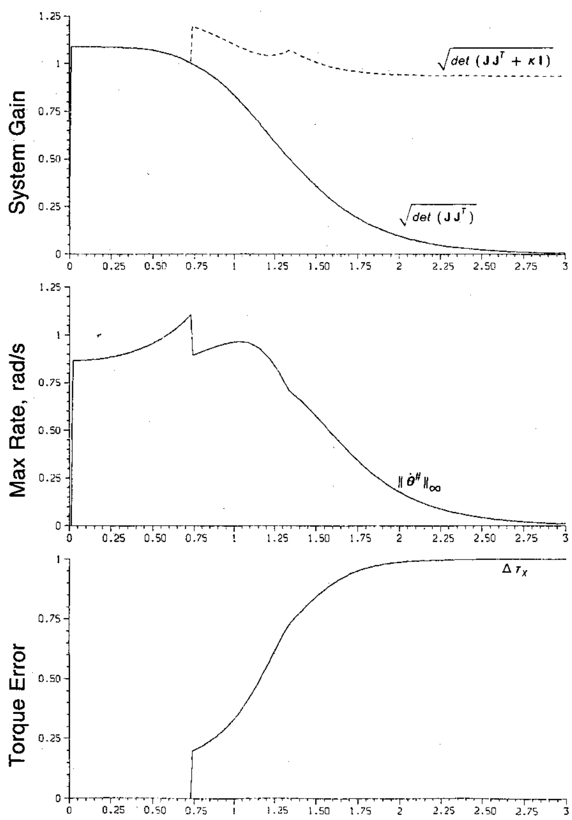

Fig. 3 Simulation results for SR-only algorithm (*X* direction).

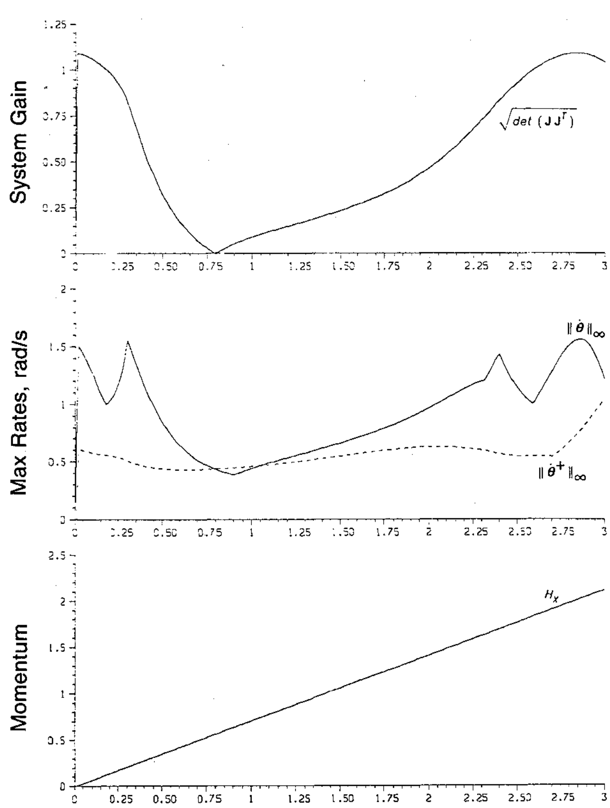

Fig. 5 Simulation results for null algorithm (*XY* direction).

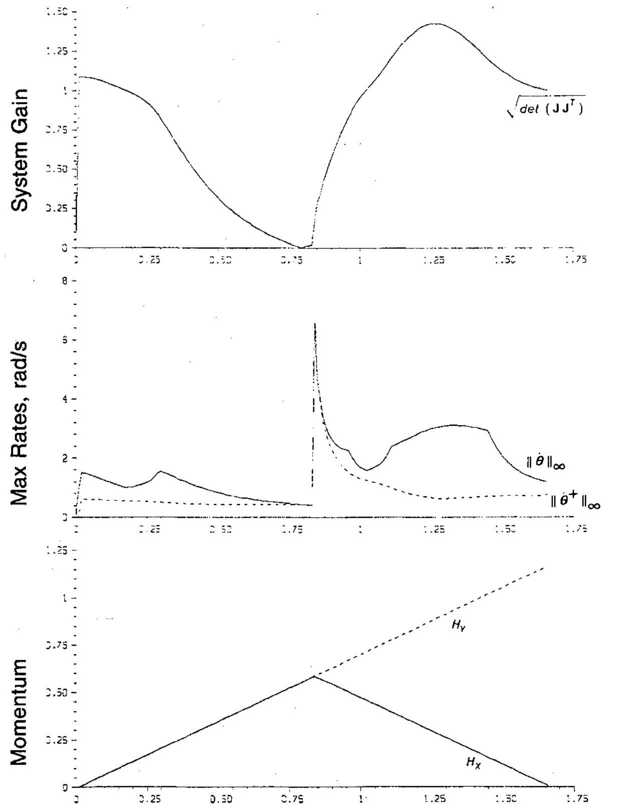

Fig. 6 **Simulation results for null algorithm (corner maneuver).**

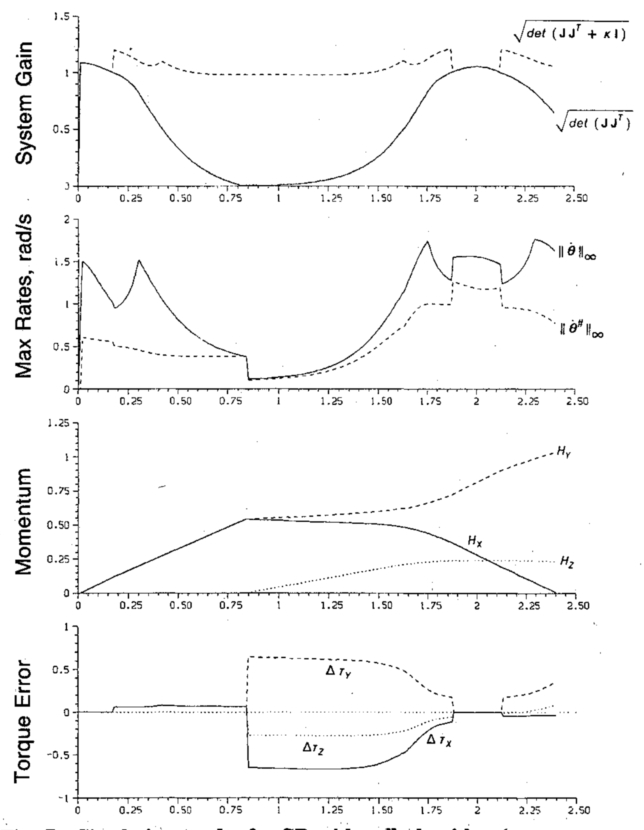

Fig. 7 **Simulation results for SR with null algorithm (corner maneuver).**

Previously, the importance of the singular direction (instead of the fact that the system is singular) was emphasized as being highly relevant to steering algorithms. It was also stated that bounded-torque-producing rates could be calculated, as long as the singular direction was orthogonal to the desired torque direction. As an example of this phenomenon, consider the unit torque request in the direction $\boldsymbol{h} = [1, 1, 0]$ shown in Fig. 5. This trajectory was generated using the nondirectional null algorithm. It is seen that the system encounters a singularity at $t = 0.8$ s, however, the gimbal rates are very well behaved.

To illustrate the adverse properties of the null algorithm of Eq. (5), another torque command was defined such that the momentum profile shown in Fig. 6 was traversed with unit torque magnitude (i.e., corner maneuver). It is clearly seen that the system becomes singular just at the switch time, causing the jump in the maximum absolute rate profile because the torque command was nearly aligned with the singular direction.

Repeating this simulation with the SR inverse using the same null motion algorithm considerably improved performance. From Fig. 7, even though the system still becomes singular, finite gimbal rates are generated because the singular direction is not exactly aligned with the torque command, allowing the system to extract itself from the singular configuration. Comparing the maximum absolute rate profiles in Fig. 6 with Fig. 7, a substantial reduction in maximum gimbal rates from over 6 rad/s for the null algorithm to less than 2 rad/s for the SR inverse is realized. The effect of the SR-induced torque error is also evident from the momentum profile, with substantial torque error occurring during the singular period. In conclusion, it is seen that the singularity is not avoided in any real sense, however, the effect of torque error coupled with the null algorithm is to generate different gimbal angle trajectories for which the singular direction is not aligned with the commanded direction.

V. Conclusion

In this paper, two steering laws, the nondirected null motion algorithm and the SR inverse, were presented as a means of avoiding internal singularities. From simulation results, the null algorithm was shown to avoid an elliptic-type singularity, whereas existing methods do not. It was also shown that elliptic-type singularities cannot be avoided using the SR inverse only. This is because the generated off-axis torque errors were not large enough to skirt the singularity, even though the magnitude of the gimbal rate solution is smaller, and the direction different from that of the pseudoinverse solution. This approach, however, was shown to provide considerably better performance when used with the nondirected null algorithm. In a corner maneuver where the null algorithm performed poorly, the SR inverse with the nondirectional null motion exhibited superior performance, albeit at the expense of substantial torque errors. The prime mechanism for singularity avoidance using the SR inverse with any null algorithm is the reduction of system response in the vicinity of a singular state. This allows for a longer time interval over which null motion can act, and consequently the effectiveness of the null solution is increased. Although the SR inverse can sometimes skirt the singular momentum state through the addition of torque error, thus avoiding a problematic gimbal angle configuration, the reduction in system response along the commanded direction coupled with the effect of null motion remains the primary mechanism for singularity avoidance.

Acknowledgments

This paper was prepared by the Charles Stark Draper Laboratory, Inc., under NASA Contract NAS9-17560. The work was supported by the NASA Johnson Space Center. Publication of this report does not constitute approval by NASA of findings or conclusions contained herein. It is published for the exchange and stimulation of ideas.

References

[1]Bedrossian, N. S., Paradiso, J., Bergmann, E. V., and Rowell, D., "Redundant Single Gimbal Control Moment Gyroscope Singularity Analysis," *Journal of Guidance, Control, and Dynamics,* Vol. 13, No. 6, pp. 1096–1101.

[2]Hogan, N., "Impedance Control: An Approach to Manipulation: Part II–Implementation," *Journal of Dynamic Systems, Measurement, and Control,* Vol. 107, March 1985, pp. 8–16.

[3]Slotine, J.-J. E., and Yoerger, D. R., "A Rule-Based Inverse Kinematic Algorithm for Redundant Manipulators," *International Journal of Robotics and Automation,* Vol. 2, No. 1, 1987.

[4]Sciavicco, L., and Siciliano, B., "A Dynamic Solution To The Inverse Kinematic Problem for Redundant Manipulators," *Proceedings of the IEEE International Conference on Robotics and Automation,* Inst. of Electrical and Electronics Engineers, New York, 1987, pp. 1081–1086.

[5]Dorny, C. N., *A Vector Space Approach to Models and Optimization,* R. E. Krieger, Malabar, FL, 1983.

[6]Schiehlen, W. O., "Two Different Approaches for a Control Law of Single Gimbal Control Moment Gyro Systems," NASA TM X-64693, Aug. 1972.

[7]Baillieul, J., Hollerbach, J., and Brockett, R., "Programming and Control of Kinematically Redundant Manipulators," *Proceedings of the 23rd Conference on Decision and Control,* Inst. of Electrical and Electronics Engineers, New York, 1984, pp. 768–774.

[8]Cornick, D. E., "Singularity Avoidance Control Laws for Single Gimbal Control Moment Gyros," *Proceedings of the AIAA Guidance and Control Conference,* AIAA, New York, 1979, pp. 255–267.

[9]Kurokawa, H., Yajima, S., and Usui, S., "A New Steering Law of a Single-Gimbal CMG System of Pyramid Configuration," *Proceedings of the Xth IFAC Symposium on Automatic Control in Space,* Toulouse, France, June 25–28, 1985, pp. 249–255.

[10]Paradiso, J., "A Highly Adaptable Steering/Selection Procedure for Combined CMG/RCS Spacecraft Control," *Proceedings of the AAS Guidance and Control Conference,* American Astronautical Society Paper 86-036, 1986, pp. 263–282; also Charles Stark Draper Lab., Cambridge, MA, CSDL-P-2653, Feb. 1986.

[11]Baillieul, J., "Kinematic Programming Alternatives for Redundant Manipulators," *Proceedings of the IEEE International Conference on Robotics and Automation,* Inst. of Electrical and Electronics Engineers, New York, 1985, pp. 722–728.

[12]Spivak, M., *Calculus on Manifolds,* W. A. Benjamin, New York, 1965.

[13]Bedrossian, N. S., "Steering Law Design for Redundant Single Gimbal Control Moment Gyro Systems," M.S.M.E. Thesis, Massachusetts Inst. of Technology, Cambridge, MA, 1987.

[14]Gantmacher, F. R., *Theory of Matrices,* Chelsea, New York, 1959.

[15]Nakamura, Y., and Hanafusa, H., "Inverse Kinematic Solutions With Singularity Robustness for Robot Manipulator Control," *Journal of Dynamic Systems, Measurement, and Control,* Vol. 108, Sept. 1986, pp. 163–171.

[16]Wampler, C., "Manipulator Inverse Kinematic Solutions Based on Damped Least-Squares Solutions," *IEEE Transactions on Systems, Man, and Cybernetics,* Vol. SMC-16, No. 1, 1986, pp. 93–101.

[17]Colburn, B. K., White, L. R., and Boland, J. S., "Some Simple CMG Steering Laws For Spacecraft Attitude Control Systems," *Proceedings of the 9th Annual Asilomar Conference on Circuits, Systems and Computers,* Pacific Grove, CA, Nov. 1975.

[18]Margulies, G., and Aubrun, J-N., "Geometric Theory of Single-Gimbal Control Moment Gyro Systems," *Journal of Astronautical Sciences,* Vol. 26, No. 2, 1978, pp. 159–191.